

Rapidity-gap and rapidity-correlation study in 400-GeV/c proton-nucleus interactions

Dipak Ghosh, Jaya Roy, Madhumita Basu, Kaushik Sengupta, Sadhan Naha,
Anuradha Bhattacharyya, and Tarit Guha Thakurta

*High Energy Physics Division, Department of Physics, Jadavpur University,
Calcutta - 700032, India*

(Received 14 October 1981)

This paper presents a detailed study of the rapidity gaps and the rapidity correlations among the relativistic particles produced in proton-nucleus interaction in emulsion at 400 GeV/c. The study includes (a) cumulative rapidity-gap distribution and hence the cluster characteristics, (b) distribution of shower width (rapidity), (c) distribution of maximum rapidity gap, and (d) two-particle rapidity correlation. The experimental data have been compared with a Monte Carlo simulation assuming an independent-emission model. The target-nucleus dependence of correlation has also been studied.

I. INTRODUCTION

The multiparticle production process in high-energy hadron-nucleus interactions is a quite complex phenomenon and its study can provide a number of unique physics opportunities that are not available from a study of hadron-hadron interactions alone. Using a nuclear target one can study the properties of hadrons at the time of their production and the space-time development of hadronic process. Although the competitive capabilities of nuclear emulsion are modest in comparison with bubble chambers for studying hadron-nucleon interactions, emulsion has gained wide acceptance as producer-detector for studying hadron-nucleus interactions. In this paper the emulsion method is used to study some important experimental characteristics of the relativistic particles produced in proton-nucleus interaction at 400 GeV/c.

The paper is organized as follows. Section II presents the experimental details. Section III presents a study of cumulative rapidity-gap distributions of the shower and hence the characteristics of the clusters. In Sec. IV we study the distribution of shower width (rapidity) and maximum rapidity gap. Lastly, in Sec. V we present a detailed study of the two-particle rapidity correlation among the relativistic particles. The experimental data have been compared with a Monte Carlo simulation assuming a simple independent-emission model to search for dynamical effects. The number of gray tracks n_g has been considered as the

main parameter to study the target-nucleus-excitation dependence of correlation.

II. EXPERIMENTAL DETAILS

In this investigation we use the data obtained from a set of photoemulsion plates (Ilford K5, 600 μm) exposed horizontally to the Fermilab 400-GeV proton beam.¹ The scanning and measurements were performed on a Leitz ortholux microscope provide with a Brower traveling stage using the following optics: 53.1 \times oil-immersion objective, and 16.8 \times ocular. The events were chosen utilizing the following criteria: (i) the beam track must be $< 2^\circ$ to the mean beam direction in the pellicle; and (ii) interaction should not be within the top or bottom 20- μm thickness of the pellicle. Further, all primary beam tracks were followed back to be sure that the events chosen did not include interactions from the secondary tracks of other interactions. The primaries originating from other interactions were observed and the corresponding events were removed from the sample. With these criteria a sample of 480 events were selected for analysis. The tracks associated with each one of the interaction are classified into the following types: (a) Shower tracks (n_s) for which $b^* < 1.4$, where b^* is the normalized blob density. (b) Gray tracks (n_g) for which $b^* \geq 1.4$ and $g^* \leq 6$, where g^* is the normalized grain density. (c) Black track (N_b) for which $g^* > 6$. The spatial emission angle of all

shower tracks in an event were obtained by measuring x , y , and z coordinates of the interaction vertex, three points on the beam track, and three points on the shower track.

III. CUMULATIVE RAPIDITY-GAP DISTRIBUTION: CLUSTER CHARACTERISTICS

It has long been recognized that the high-energy multiparticle production is a two-step process,²⁻⁴ the production of highly excited hadronic states (cluster) which afterwards decay into hadrons. There are many interesting hypotheses regarding the nature of clusters, like droplet of gluons,³ resonances,^{5,6} collective phenomenon without dynamical significances,^{7,8} and excited hadronic states.⁹⁻¹¹ However there is no conclusive evidence in favor of any of these theories. Further detailed experimental information at different energies are essential to arrive at a confident conclusion about cluster.

One can study the existence of clustering in high-energy multiparticle production through rapidity-gap distributions. The rapidity Y is defined as

$$Y = \frac{1}{2} \ln(E + p_{\parallel}) / (E - p_{\parallel}), \quad (1)$$

where E and p_{\parallel} are the energy and longitudinal momentum of the shower particles, respectively. Since shower particles are primarily pions with a mean transverse momentum of ~ 0.4 GeV/ c , $p_{\parallel}^2 \gg p_T^2 \gg m^2$ (p_T and m denote the transverse momentum and mass, respectively), so that Eq. (1) becomes $Y = -\ln \tan \theta / 2$, where θ is the spatial emission angle.

The existence of clustering is indicated if there is an excess of small rapidity gaps, as compared to an exponential distribution which is expected if particles occur randomly in rapidity. Although some works have been done to study clustering by the two-particle rapidity-gap distribution in high-energy hadronic collisions, there are no significant works where higher-order clustering has been studied. In this paper, a study has been made on rapidity correlations for any arbitrary number of particles.

We represent the charged secondary particles (designated by strokes) for an event in rapidity space as in Fig. 1. We would not consider the particles at the two ends of the rapidity space since they constitute the leading and target particles. We want to study only the nondiffractive com-

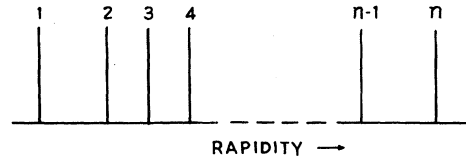


FIG. 1. Schematic representation of charged secondary particles in rapidity space.

ponent of the cross section. For a group of n charged particles adjacent in rapidity, the sum of $n - 1$ consecutive rapidity-gap lengths is

$$r(n) = Y_{i+n-1} - Y_i,$$

where Y_i is the rapidity of the first particle, i.e., the particle with lowest value of rapidity of the n -particle group. This may be termed the cumulative rapidity-gap-length variable. One can study n -particle ($n=2,3$) clustering from the experimental distribution of the cumulative rapidity-gap-length variable $r(n)$. As mentioned earlier, clustering will be evident if there is a peak in the distribution of $r(n)$ for small rapidity gaps. For all interactions the cumulative rapidity-gap lengths were calculated for $n=2,3,4,5$.

The observed inclusive distributions of $r(n)$ are shown in the figures. Figure 2 shows the distribution of $r(2)$. The sharp peak in the distribution for low values of r clearly indicate the existence of a two-particle correlation. Figure 3 shows a similar sharp peak in the distribution of $r(3)$, indicating the existence of a three-particle correlation.

No sharp peak is observed in the distribution of $r(4)$ and $r(5)$ (Fig. 4). Hence higher-order correlations do not exist in these interactions. These distributions can be represented by the equations of

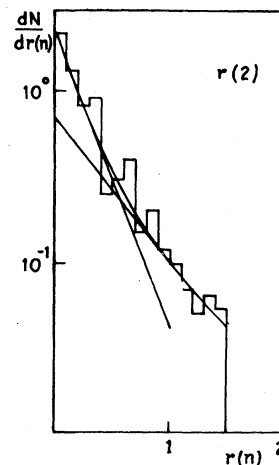


FIG. 2. Distribution of rapidity-gap length $r(2)$.

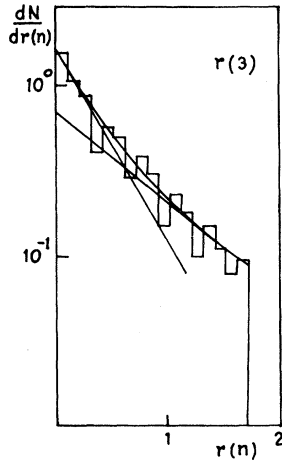


FIG. 3. Distribution of cumulative rapidity-gap length $r(3)$.

the form

$$\frac{dn}{dr} = Ae^{-Br} + Ce^{-Dr}.$$

It has been shown in some works that the two-particle rapidity-gap distribution in high-energy hadron collisions follows the form given in Eq. (1). It is interesting to note that here also the distribution of $r(2)$ and $r(3)$ also follow the same form. The numerical equations of the theoretical curves represented by the solid line in Figs. 2 and 3 are, respectively,

$$\frac{dn}{dr(2)} = 8.16e^{-7.85} + 2.01e^{-0.84}, \quad (2)$$

$$\frac{dn}{dr(3)} = 6.04e^{-4.47} + 1.97e^{-0.66}. \quad (3)$$

(The fits have been performed by the CERN optimization program MINUIT, the details of which are given in Table I.)

The contributions of the two individual terms in Eqs. (2) and (3) are also shown in the figures. The fast decreases at the small values of $r(n)$ and slow at large values signifies the presence of short-range and long-range correlations, respectively. It is apparent from the result of this analysis that the

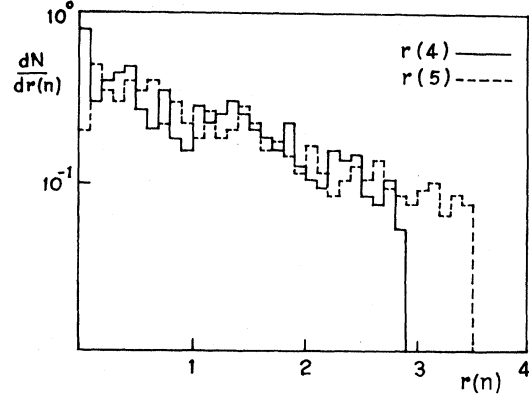


FIG. 4. Distribution of cumulative rapidity-gap length $r(4)$ (solid) and $r(5)$ (dashed).

main contribution to the term $dN/dr(n)$ comes from the short-range correlation.

The value of the slope B provides a measure of the strength of the correlation in the first region of rapidity difference distribution. The reason is obvious. The more closely the particles are spaced in rapidity, the smaller is the rapidity difference, and consequently the slope of the rapidity difference distribution will increase. In other words, the greater the number of small values of rapidity difference, the larger the value of the slope and hence the correlations. The strength of the correlation will indicate whether the cluster production is the predominant mode of particle production or not. We find from Eqs. (3) and (4) that with the increase in the number of particles in a cluster, the strength of the correlation tends to decrease. Further, from the above equations, we find that the value of the slope D in the second term maintains more or less a constant value. This signifies the independent emission of particles contributing in that part of the $r(n)$ distribution. These observations are in agreement with the results at other energies.^{12,13}

Thus we conclude from this analysis of the cluster characteristics by the generalized rapidity-gap distribution that both two-particle and three-

TABLE I. Details of the fits to rapidity-gap distribution.

	A	B	C	D	χ^2/DF
Two particles	8.16 ± 0.85	7.85 ± 0.52	2.01 ± 0.25	0.84 ± 0.09	0.7
Three particles	6.04 ± 0.50	4.47 ± 0.39	1.97 ± 0.14	0.66 ± 0.04	0.8

particle clusters are present in 400-GeV/ c p -nucleus interactions, and the strength of the correlation tends to decrease with an increase of cluster mass.

IV. SHOWER-WIDTH AND MAXIMUM-RAPIDITY-GAP DISTRIBUTIONS

In this section we shall consider first the distribution of the widths of the relativistic charged particles shower (R), which is defined as the difference between the highest and the lowest ordered rapidity in an event, i.e., $R = Y_n - Y_1$, for an event of multiplicity n . Figure 5 shows the distribution of R for 400 GeV/ c p -emulsion interaction. It is interesting to compare this with the data at other momenta, namely 70, 200, and 300 GeV/ c . It is observed that the nature of the distribution is identical with a central prominent peak at all energies, which indicates that the same fundamental process is responsible for the production of the shower at energies concerned.

Another important characteristic which deserves special interest is the maximum-rapidity-gap distribution. The maximum rapidity gap Δ_{\max} is defined to be the maximum value of the rapidity gap between adjacent charged particles, in an event when ordered according to their rapidity values, i.e.,

$$\Delta_{\max} = \max(Y_{i+1} - Y_i).$$

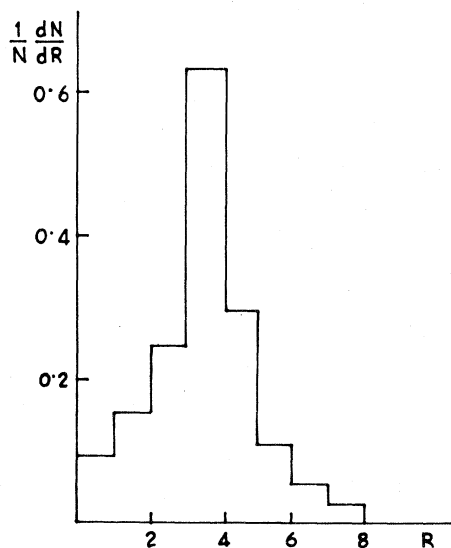


FIG. 5. Distribution of shower width of relativistic charged particles.

From the study of the Δ_{\max} distribution, one hopes to get information about the nature of the particle-production process. The diffractive processes are expected to contribute mainly to large values of Δ_{\max} , whereas the nondiffractive ones would contribute very little to that region of Δ_{\max} . Jones and Snider¹⁴ have proposed a method of determining the amount of diffractive dissociation based on the distribution of the maximum rapidity gap. They have obtained the distribution from a multiperipheral model by taking into account the exchange of Reggeons and Pomerons, and found that the Δ_{\max} distribution is dominated by diffractive dissociation for $\Delta_{\max} > 4.0$. A few cases have been reported where study of the Δ_{\max} distribution has been made in the case of hadron-hadron interaction. However, no such study has been made in the case of hadron-nucleus collision. We present our experimental data on the characteristics of the distribution in proton-emulsion interaction of 400 GeV and compare it with theoretical predictions of Jones and Snider.

Figure 6 shows the experimental Δ_{\max} distribution along with the theoretical prediction. The solid curve indicates the prediction according to

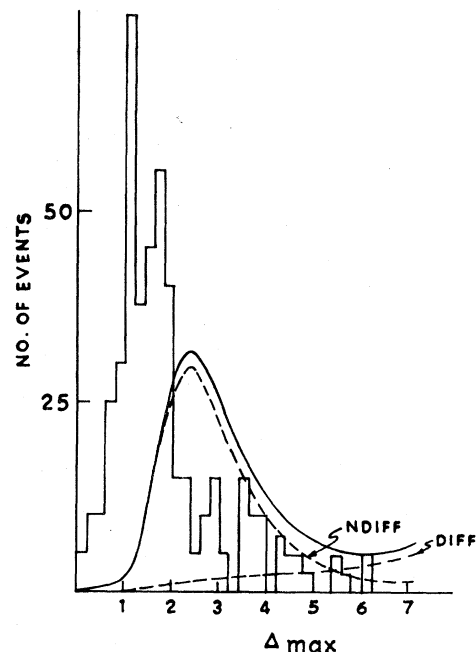


FIG. 6. Distribution of the maximum rapidity interval Δ_{\max} .

Jones and Snider. The dashed curves (1) and (2) are the break up of the solid curves into diffractive and nondiffractive parts.

The following are the conclusions that can be drawn from the comparison of the experimental points and the theoretical curves.

(1) There is a prominent peak in the small- Δ_{\max} region due to nondiffraction production and the distribution falls off.

(2) The peak in the experimental distribution falls in the region of $\sim 1.0-1.2$ and this is shifted significantly with respect to the theoretical distribution towards the region of small Δ_{\max} .

(3) A few events have been observed which are due to Pomeron exchange, i.e., due to fragmentation of the interacting particles. It is observed that the number of such events is smaller than the theoretical predictions and there is no indication of the existence of a pure diffractive peak at large values of Δ_{\max} as predicted.

The shift of the experimental peak towards the region of small Δ_{\max} with respect to the theoretical distribution can, however, be explained by the correlation of secondary particles.

$$C(Y_1, Y_2, p_{T1}, p_{T2}, s, A) \equiv \frac{1}{\sigma_{\text{in}}} \frac{d^6\sigma}{dY_1 dY_2 d^2p_{T1} d^2p_{T2}} - \left[\frac{1}{\sigma_{\text{in}}} \right]^2 \frac{d^3\sigma}{dY_1 d^2p_{T1}} \frac{d^3\sigma}{dY_2 d^2p_{T2}},$$

where Y represents the rapidity, p_T the transverse momentum, A the mass number, and s the squared c.m. energy; the subscripts, 1 and 2 stand for the two particles considered. Integrating over p_T one gets

$$C(Y_1, Y_2, s, A) \equiv \frac{1}{\sigma_{\text{in}}} \frac{d^2\sigma}{dY_1 dY_2} - \left[\frac{1}{\sigma_{\text{in}}} \right]^2 \frac{d\sigma}{dY_1} \frac{d\sigma}{dY_2},$$

where

$$\begin{aligned} \frac{1}{\sigma_{\text{in}}} \int \frac{d^2\sigma}{dY_1 dY_2} dY_1 dY_2 &= \langle n_s(n_s - 1) \rangle, \\ \frac{1}{\sigma_{\text{in}}} \int \frac{d\sigma}{dY} dY &= \langle n_2 \rangle, \\ \int C dY_1 dY_2 &= f_2. \end{aligned}$$

f_2 is the multiplicity moment defined as

$$f_2 = \langle n_s(n_s - 1) \rangle - \langle n_2 \rangle^2.$$

V. TWO-PARTICLE RAPIDITY CORRELATION

From a study of correlation among produced particles in hadronic interactions at high energy, one hopes to get important information about the multiparticle production mechanism and the quark structure of hadrons.¹⁴⁻¹⁶ Since the single-particle distribution is less sensitive to the choice among the various models of particle production, it is essential to investigate multiparticle (correlation) effects. Although some works have been devoted to such investigations, in most of them no search has been made for true dynamical correlation.^{17,18}

Here we present detailed data on the two-particle rapidity correlation in proton-emulsion interaction at 400 GeV/c; a comparison of the data with Monte Carlo simulation has been made to search for the dynamical correlation. Also we study the target-nucleus-excitation dependence of the correlation using n_g (number of gray particles) as the main parameter.

A general two-particle correlation function has been defined as¹⁹

We choose pseudorapidity (η) in c.m. as a variable:

$$\eta = \eta_L - \ln[\gamma_c(1 + \beta_c)],$$

where $\eta_L = -\ln \tan \theta/2$ is the pseudorapidity in the laboratory frame, θ is the emission angle of the produced particle with respect to the incident beam, and $\gamma_c = (1 - \beta^2)^{-1/2}$ is the Lorentz factor of the pp collision with the proton target at rest.

Since the shower particles are primarily pions with mean $p_T \sim 0.4$ GeV/c, $p_{\parallel}^2 \gg p_T^2 \gg m^2$ for most of the particles, η_L closely approaches the laboratory rapidity

$$Y = \frac{1}{2} \ln \frac{E + p_{\parallel}}{E - p_{\parallel}}.$$

The correlation function C then becomes

$$\begin{aligned} C(\eta_1, \eta_2) &= \frac{1}{\sigma_{\text{in}}} \frac{d^2\sigma}{d\eta_1 d\eta_2} - \frac{1}{\sigma_{\text{in}}^2} \frac{d\sigma}{d\eta_1} \frac{d\sigma}{d\eta_2} \\ &= \frac{N_2(\eta_1, \eta_2)}{N} - \frac{N_1(\eta_1)N_1(\eta_2)}{N^2}, \end{aligned}$$

where $N_1(\eta)$ is the number of shower particles with pseudorapidity between η and $\eta+d\eta$; $N_2(\eta_1, \eta_2)$ is the number of pairs of shower particles with pseudorapidity between η_1 , $\eta_1+d\eta_1$, and

η_2 , $\eta_2+d\eta_2$ in the same event, and N is the total number of inelastic interactions in the sample.

Further the normalized correlation function R can be defined as

$$R(\eta_1, \eta_2) = \frac{(1/\sigma_{in})(d^2\sigma/d\eta_1 d\eta_2) - (1/\sigma_{in}^2)(d\sigma/d\eta_1)(d\sigma/d\eta_2)}{(1/\sigma_{in}^2)(d\sigma/d\eta_1)(d\sigma/d\eta_2)} = \frac{NN_2(\eta_1, \eta_2)}{N_1(\eta_1)N_1(\eta_2)} - 1.$$

A. Monte Carlo simulation

In the study of correlations by means of correlation functions, pseudocorrelations arise from the broad multiplicity distribution and the dependence of the one-particle spectrum on multiplicity, as well as the trivial correlations due to kinematical constraints in individual events. Although, as has been emphasized earlier, the precise model-independent search for dynamical correlations seems to be impossible in hadron-nucleus interactions, some attempts can be made to deal with this problem by comparing the correlation data with calculations performed by the Monte Carlo method in the framework of the independent-emission hypothesis using the following assumptions: (a) the emission angle of shower particles are independent statistically; (b) multiplicity distribution $d\sigma/dn$ in Monte Carlo events reproduces the empirical multiplicity spectrum of the real ensemble; and (c) the one-particle spectrum $d\sigma/d\eta$ in the simulated interactions reproduces the empirical semi-inclusive distribution $d\sigma/\eta d\eta$, with the corresponding n_s for the real ensemble. It has been shown by Gulamov *et al.*²⁰ and also by us²² from a comparison of correlation functions calculated in the random stars generated according to the cylindrical-phase-space (CPS) model and the independent-emission model (IEM) (which has been used here), that the conservation laws lead to the increase of long-range correlations and to the decrease of short-range correlations, especially in the beam fragmentation region. Hence one can conclude that any observation of an excess short-range correlation over the Monte Carlo—simulated value (here) will indicate the presence of dynamical effects and cannot be explained by conservation laws. Thus by comparing correlation functions C and R obtained from the experiment with those C_M and R_M obtained from Monte Carlo simulation, one can search for the dynamical correlation.

Let us denote

$$C_D = C - C_M,$$

$$R_D = R - R_M.$$

C_D and R_D can be interpreted to a good extent as manifestations of dynamical correlations.

B. Target-nucleus-excitation dependence of correlation functions C and R

The aim of studying the interactions of hadrons with nuclear targets is to test primarily the ν dependence of the production process (ν stands for the number of inelastic collisions of the incident hadron with the nucleons of the nucleus). One can control the distribution by changing the size of the

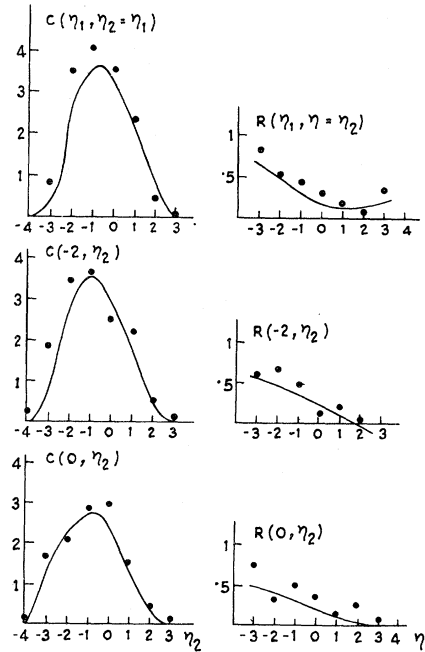


FIG. 7. Different correlation functions $C(\eta_1, \eta_2)$ and $R(\eta_1, \eta_2)$ for p -emulsion interaction at 400 GeV/c. Monte Carlo values $C_M(\eta_1, \eta_2)$ and $R_M(\eta_1, \eta_2)$ are indicated by solid curves.

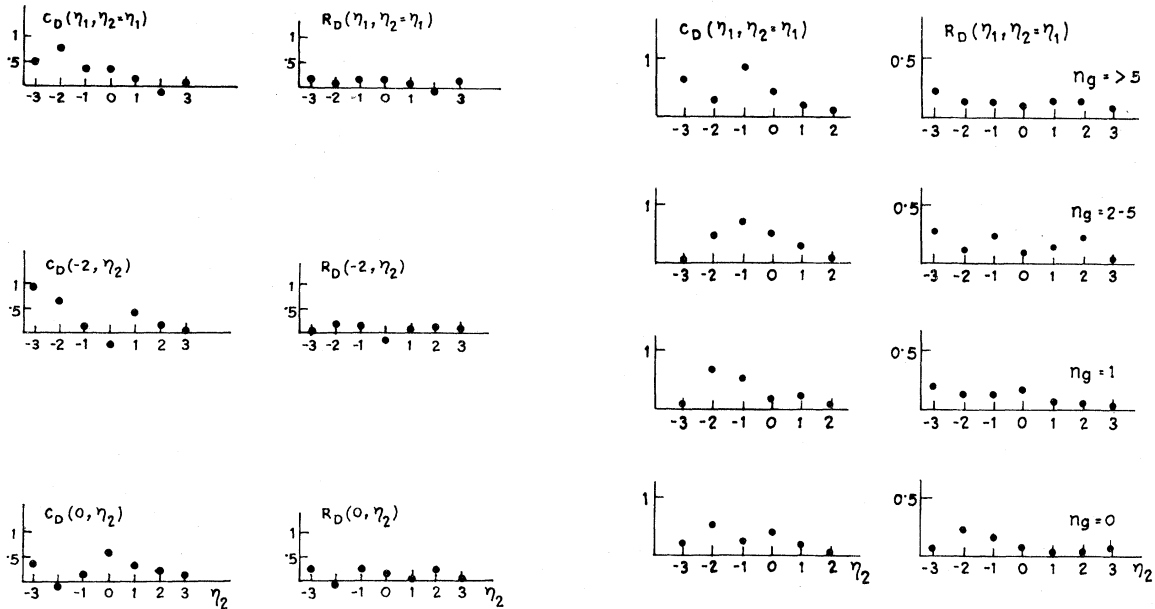


FIG. 8. "Dynamical surplus" C_D and R_D for the cases shown in Fig. 7.

nucleus or by selecting the number of events with some fixed degree of the excitation of target nucleus. In this respect a very useful parameter is the number of gray tracks (n_g) accompanying the production process. It has been shown recently²⁰

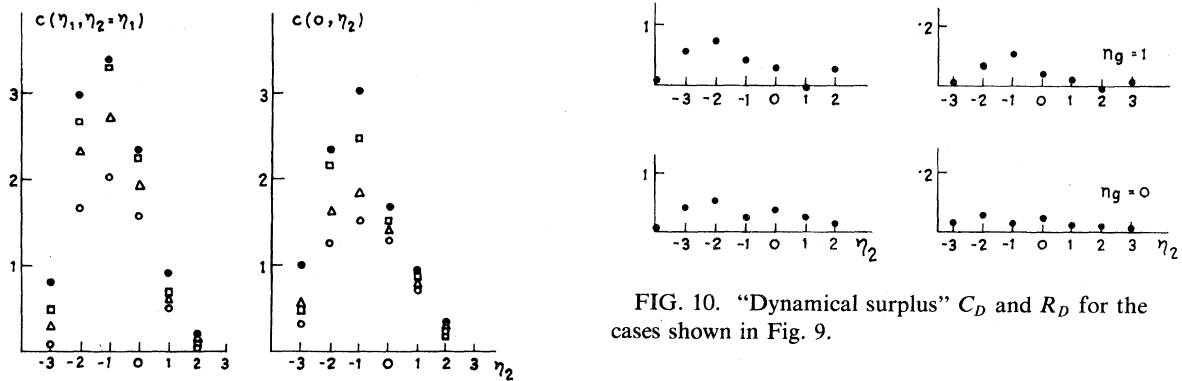


FIG. 9. Different correlation functions $C(\eta_1, \eta_2)$ and $R(\eta_1, \eta_2)$ for different n_g groups.

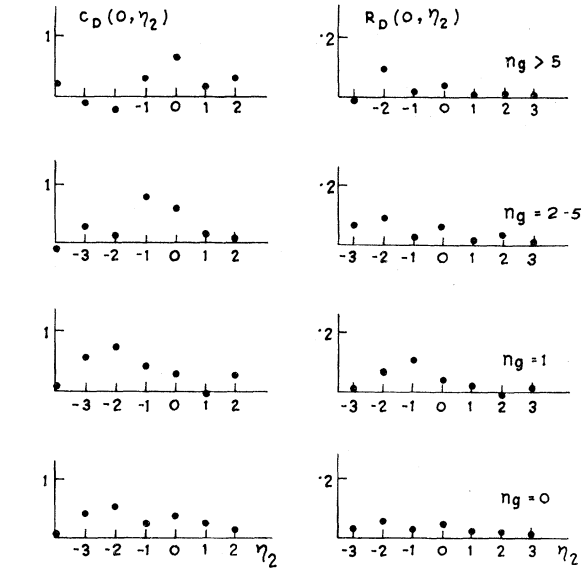


FIG. 10. "Dynamical surplus" C_D and R_D for the cases shown in Fig. 9.

how n_g measures the number of collisions inside the nucleus. Apart from the exact relationship between ν and n_g , the results which are important in this context are (a) small values of n_g which correspond obviously to the peripheral interactions (the correlation functions in those cases are expected then to be similar to those for nucleus and light nuclei), (b) very large values of n_g which correspond to the maximum possible values of ν .

In view of the discussion above, it is worthwhile to study the n_g dependence of the correlation func-

tions C and R . The two-particle correlation functions C and R for relativistic particles produced in p -emulsion interactions at 400 GeV/ c , along with the Monte Carlo—simulated values, are shown in Fig. 7. Figure 7(a) presents the correlation functions $C(\eta_1, \eta_2 = \eta_1)$ and $R(\eta_1, \eta_2 = \eta_1)$, i.e., the values of the diagonal element of the correlation metrics, characterizing the magnitude of “short-range” correlations at different η . Figures 7(b) and 7(c) show the rows $C(-2, \eta)$, $R(-2, \eta)$ and $C(0, \eta)$, $R(0, \eta)$. Figure 8 shows the corresponding values for the “dynamical surplus” C_D and R_D . The following are the conclusions.

(i) The graph clearly reveals the existence of positive short-range correlations among the relativistic particles.

(ii) This correlation is most prominent in the central region.

(iii) This correlation cannot be explained by the simplest trivial and kinematical factors.

(iv) Long-range correlations are not visible, although it is not justified to exclude the possibility of some long-range correlating behavior from the statistics of this experiment.

In order to study the dependence of the correlation function on the number of gray particles (n_g), we divide the data into different n_g groups, namely,

$$n_g = 0, 1, 2-5, > 5$$

and calculate the correlation functions C and R in

each case.

The values of the correlation functions $C(\eta_1, \eta_2 = \eta_1)$, $R(\eta_1, \eta_2 = \eta_1)$ and $C(0, \eta)$, $R(0, \eta)$ for different n_g groups have been shown in Fig. 9 (the Monte Carlo values are not shown to avoid clumsiness). Figure 10 shows the corresponding dynamical surplus.

The most important conclusions that can be made are the following.

(1) The shapes of the correlation functions in different groups of n_g are more or less similar.

(2) The value of C increases, whereas R decreases with increasing n_g , which can be explained in the following way.

Due to possible correlations between n_s and n_g ,^{21,22} the effect of conservation laws becomes less with increasing n_g , and consequently the underestimation of C_D and R_D (for using this Monte Carlo simulation for C_M and R_M , as has been discussed earlier) increases with decreasing n_g . Thus C_D and R_D indicate that the correlations decrease with increasing n_g . It deserves mention that this decrease of R with increasing n_g favors the prediction of the additive quark model²³ among the recent models of the particle-production mechanism.

ACKNOWLEDGMENT

The authors would like to thank Professor P. L. Jain, State University of New York at Buffalo, for kindly sending the exposed emulsion plates.

¹D. Ghosh *et al.*, contributed to the XX International Conference on High Energy Physics, Madison, Wisconsin, 1980 (unpublished).
²S. Pokorski and V. Van Hove, *Acta Phys. Pol.* **B5**, 229 (1974).
³P. Pirva and S. Pokorski, *Phys. Lett.* **43B**, 503 (1973).
⁴H. Satz, *Acta Phys. Pol.* **B5**, 3 (1974).
⁵A. Gula, in *High Energies and Elementary Particles*, Proceedings of the International Symposium, Warsaw, 1975 (JINR, Dubna, 1975), p. 108.
⁶A. Arneodo and G. Plant, *Nucl. Phys.* **B107**, 262 (1976).
⁷A. Krzywicki, in *Proceedings of the Colloquium on Hadronic Physics at ISR Energies, Marseille, 1973*, edited by J. Soffer (Centre de Physique Theorique, Marseille, 1974), p. 13.
⁸J. Karcsmaremuk, *Nucl. Phys.* **B78**, 370 (1974).
⁹R. Hagedorn, *Nuovo Cimento Suppl.* **3**, 147 (1965).
¹⁰S. Frautschi, *Phys. Rev. D* **3**, 2821 (1971).
¹¹I. Montvay, *Phys. Lett.* **42B**, 466 (1972).
¹²D. Ghosh, *Ann. Phys. (Leipzig)* **37**, 155 (1980); D.

Ghosh *et al.*, *Ind. J. Pure Appl. Phys.* **18**, 544 (1980); *Can. J. Phys.* **57**, 2036 (1979); *Proc. Phys. Soc. J.* **50**, 2709 (1981).
¹³D. Ghosh *et al.* (unpublished).
¹⁴S. T. Jones and D. R. Snider, *Phys. Rev. D* **9**, 242 (1974).
¹⁵A. Dar and J. Vary, *Phys. Rev. D* **6**, 2412 (1973).
¹⁶L. Bergström and S. Fredriksson, *Phys. Lett.* **78B**, 337 (1978).
¹⁷E. M. Levin *et al.*, *Z. Phys. C* **5**, 285 (1980).
¹⁸G. Baroni *et al.*, *Nucl. Phys.* **B103**, 213 (1976); *Lett. Nuovo Cimento* **18**, 352 (1977); J. M. Bolts *et al.*, *Nuovo Cimento* **59A**, 773 (1980).
¹⁹W. R. Frazer *et al.*, *Rev. Mod. Phys.* **44**, 284 (1972); H. Boggild and T. Ferbal, *Annu. Rev. Nucl. Sci.* **24**, 451 (1974).
²⁰K. G. Gulamov *et al.*, *Z. Phys. A* **280**, 107 (1977).
²¹B. Anderson *et al.*, *Phys. Lett.* **73B**, 349 (1978).
²²Dipak Ghosh *et al.* (unpublished).
²³N. N. Nikolaev and A. Ya. Ostapchuk, CERN Report No. Ref. TH-2575-CERN, 1978 (unpublished).